

## Virtual Simulation System with Path-Following Control for Lunar Rovers Moving on Rough Terrain

GAO Haibo DENG Zongquan DING Liang\* WANG Mengyu

1 State Key Laboratory of Robotics and Systems, Harbin Institute of Technology, Harbin 150001, China

2 School of Mechatronics, Harbin Institute of Technology, Harbin 150001, China

Received June 1, 2010; revised May 9, 2011; accepted May 13, 2011; published electronically May 18, 2011

**Abstract:** Virtual simulation technology is of great importance for the teleoperation of lunar rovers during the exploration phase, as well as the design of locomotion systems, performance evaluation, and control strategy verification during the R&D phase. The currently used simulation methods for lunar rovers have several disadvantages such as poor fidelity for wheel-soil interaction mechanics, difficulty in simulating rough terrains, and high complexity making it difficult to realize mobility control in simulation systems. This paper presents an approach for the construction of a virtual simulation system that integrates the features of 3D modeling, wheel-soil interaction mechanics, dynamics analysis, mobility control, and visualization for lunar rovers. Wheel-soil interaction experiments are carried out to test the forces and moments acted on a lunar rover's wheel by the soil with a vertical load of 80N and slip ratios of 0, 0.03, 0.05, 0.1, 0.2, 0.3, 0.4 and 0.6. The experimental results are referenced in order to set the parameters' values for the PAC2002 tire model of the ADAMS/Tire module. In addition, the rough lunar terrain is simulated with 3DS Max software after analyzing its characteristics, and a data-transfer program is developed with Matlab to simulate the 3D reappearance of a lunar environment in ADAMS. The 3D model of a lunar rover is developed by using Pro/E software and is then imported into ADAMS. Finally, a virtual simulation system for lunar rovers is developed. A path-following control strategy based on slip compensation for a six-wheeled lunar rover prototype is researched. The controller is implemented by using Matlab/Simulink to carry out joint simulations with ADAMS. The designed virtual lunar rover could follow the planned path on a rough terrain. This paper can also provide a reference scheme for virtual simulation and performance analysis of rovers moving on rough lunar terrains.

**Key words:** lunar rover, comprehensive simulation system, rough terrain, wheel-soil interaction mechanics, path-following control

### 1 Introduction

With the upsurge in lunar exploration missions using lunar rovers that started in the 1990s, China's Chang'e lunar exploration project plans to launch a rover to the moon in 2013.

Virtual simulation can be used to guarantee the success of a lunar rover, since it can provide a platform for optimal design, evaluation, and control, during the R&D phase, and can also support 3D predictive displays for continuous teleoperation or command-sequence validation, during the exploration phase<sup>[1]</sup>.

In this regard, a comprehensive virtual simulation system that combines the features of 3D modeling, dynamics analysis, control, and visualization, is becoming popular.

The *Jet Propulsion Laboratory (JPL)* of the *USA* has developed ROAMS (Rover Analysis Modeling and Simulation Software) for the development of Mars rovers<sup>[2]</sup>, which can be used for joint simulation with a double-layer software framework for the autonomous control called CLARAty (Coupled Layer Architecture for Robotic Autonomy) to verify control strategies. ROAMS, CLARAty, and WITS (The Web Interface for Telescience, a science operations tool for downlink data visualization and uplink science activity after verification by simulation) are three complementary infrastructure elements funded by the *Mars Technology Program* in conjunction with the *Mars Science Laboratory Mission of NASA*<sup>[3]</sup>. *ESA* is planning to send a Mars exploration rover called ExoMars to search for signs of life on Mars. RCET (Rover Chassis Evaluation Tool), which consists of a 2D rover simulator, was jointly developed by a number of European institutions, including *Contraves Space*, *EPFL*, *DLR*, to support the design of planetary rovers<sup>[4]</sup>. They also developed RPET (Rover Performance Evaluation Tool), which is similar to the RCET<sup>[5]</sup>. RCAST was developed in order to characterize and optimize the mobility of the ExoMars rover and evaluate the locomotion subsystem before RCET is ready.

\* Corresponding author. E-mail: liangding@hit.edu.cn

This project is supported by National Natural Science Foundation of China (Grant No. 50975059/61005080), Postdoctoral Foundation of China (Grant No. 20100480994), Postdoctoral Foundation of Heilongjiang Province, Foundation of Chinese State Key Laboratory of Robotics and Systems (Grant No. SKLRS200801A02), and College Discipline Innovation Wisdom Plan of China (111 Project, Grant No. B07018)

It can also be used to carry out the joint simulation based on the Matlab SimMechanics toolbox and virtual reality toolbox using an interface with CAD modeling software<sup>[6]</sup>.

The simulation of rover dynamics is mainly concerned with the terramechanics of wheel-soil interaction and multi-rigid-body dynamics. Terramechanics presents the largest obstacle to the enhancement of simulation fidelity. A simple Hunt-Crossley spring damping model<sup>[7]</sup> or Bekker's conventional terramechanics models<sup>[5]</sup> for terrestrial vehicles are used in the abovementioned simulation tools. These models, however, cannot very well reflect the dynamics of wheels moving on a rough, deformable lunar terrain, which results in low fidelity simulation.

General dynamics simulation software such as ADAMS and DADS are usually used by Chinese researchers to simulate and analyze the motion of lunar rover prototypes through the use of embedded "contact" models<sup>[8-10]</sup>. LIANG, et al of *Beijing Institute of Control Engineering* has discussed technical approaches for designing lunar rovers, including the development of a comprehensive simulation platform<sup>[11]</sup>. A joint simulation method for lunar rovers using DADS and Matlab is presented in Ref. [12]. The architecture of a comprehensive high-speed/high-fidelity simulation platform for lunar rovers has also been designed, and its key relevant techniques have been analyzed<sup>[1]</sup>. The currently used simulation methods for lunar rovers have several disadvantages such as poor fidelity for wheel-soil interaction mechanics, difficulty in simulating rough terrains, and high complexity making it difficult to realize mobility control in simulation systems.

## 2 Structure of Comprehensive Virtual Simulation System for Lunar Rovers

The structure of a comprehensive virtual simulation system for lunar rovers is shown in Fig. 1. The simulation system integrates the software of PRO/E, 3DS Max, ADAMS, and Matlab to realize the functions of rover vehicle modeling, terrain modeling, kinematics/dynamics analysis including the mechanics of wheel-soil interaction, and control, respectively.

The 3D model of a lunar rover that is constructed by using Pro/E can be imported into ADAMS through an ADAMS/Pro connection module; the rough terrain model of the lunar surface formed with 3DS Max can be imported into an ADAMS/Tire module through an interface for them; the PAC2002 tire model is called by the ADAMS/Tire module for prediction of the terramechanics of the wheel-soil interaction. By configuring the simulation parameters for the rover model, the terrain and tire model in ADAMS, a virtual rover is constructed, whose kinematics and dynamics can be solved by ADAMS/Solver.

In order to direct a virtual rover to follow a planned path while compensating for slipping on deformable rough terrain, the required control strategy can be realized with Matlab. A virtual rover created by ADAMS software can be

controlled through the interface between ADAMS/Control and Matlab/Simulink. ADAMS/Control provides an interactive environment for establishing and demonstrating an S-function "controlled object," which can be controlled by the Simulink toolbox of Matlab. In each integration step, ADAMS/Control is called as a subprogram by Simulink. The control instructions generated by Simulink are then directed to the corresponding mechanisms (such as the driving motors of the wheels) of lunar rovers in ADAMS through ADAMS/Control. The rover's motion is then calculated by ADAMS/Solver based on dynamics simulation, and the related information is fed back to Simulink through ADAMS/Control. The entire transmission process is automatic and transparent.

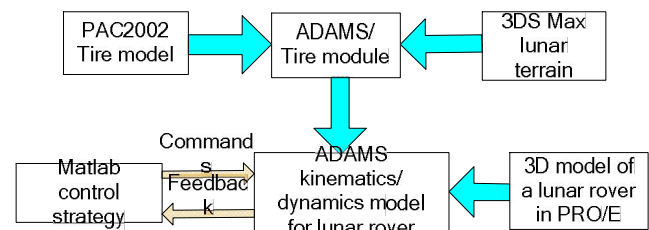


Fig. 1. Diagram of comprehensive virtual simulation system for lunar rovers

## 3 Tire Model for Predicting Wheel-Soil Interaction Mechanics

### 3.1 Analysis and selection of ADAMS/Tire model

The fidelity of lunar rover simulation primarily lies in the precision of the mathematic models used for predicting the dynamics between a wheel and the soft lunar soil. When using ADAMS to carry out simulations for lunar rovers locomotion systems, researchers usually presume that the lunar surface is rigid, and accordingly use a contact model for rigid bodies by modulating the static and dynamic frictional coefficients. This method, however, does not accurately reflect the interaction between the rover's wheels and soft soil, and what makes this method even worse, very rough terrain cannot be realized since the terrain is treated as a composition of structured rigid objects.

ADAMS/Tire is a module for predicting the interactive forces and moments between wheels and roads. Several types of tire models are provided by ADAMS, including MF-Tyre, UA, Ftire, SWIFT, PAC89, and PAC2002. Each tire model has its own advantages and disadvantages. After careful analysis and comparison, the PAC2002 model was finally chosen for calculation of the mechanics of wheel-soil interaction of a lunar rover. This model is applicable to the interaction between a wheel and 3D roads or obstacles.

The PAC2002 model uses trigonometric functions to fit the experimental data in order to predict the forces and moments that the soil exerts upon a wheel, including the

drawbar pull  $F_x$ , lateral force  $F_y$ , sustaining force  $F_z$ , overturning moment  $M_x$ , resistance torque  $M_y$ , and aligning torque  $M_z$ . The general expression of the function, which is called the magic formula, is

$$Y(X) = D \cos(C \arctan\{BX - E[BX - \arctan(BX)]\}), \quad (1)$$

where  $Y(X)$  is a force or moment, the independent variable  $X$  reflects the effect of the slip angle or longitudinal slip ratio of a wheel for an actual situation, parameters  $B$ ,  $C$ , and  $D$  are determined by the wheel's vertical load and camber angle, while  $E$  is the curvature factor. The unknown parameters can be determined by a data fitting method based on experimental results.

Once the parameters of the magic formula are identified based on experimental data, the PAC2002 model can predict wheel-soil interaction mechanics with a high degree of accuracy under the experimental conditions; the model also has a high degree of confidence beyond the limited experimental conditions.

### 3.2 Experimental study of wheel-soil interaction mechanics

Fig. 2 shows the test-bed for the study of wheel-soil interaction mechanics that was developed in the authors' laboratory. The test-bed is equipped with a 6-axis F/T sensor, a displacement sensor, a driving torque sensor, encoders, etc. It can be used to test the forces and moments that act upon an experimental wheel that come from the soil, wheel sinkage, driving torque, etc. The longitudinal slip ratio of a wheel that can be modulated by coordinating the velocity of the driving motor and carriage motor has a great influence on wheel-soil interaction.



Fig. 2. Wheel-soil interaction test-bed

Experiments were performed by using a lunar soil simulant to investigate wheel-soil interaction performance. The vertical load was 80 N, and the slip ratios were set to 0, 0.03, 0.05, 0.1, 0.2, 0.3, 0.4, and 0.6. The lunar regolith simulant was provided by *Shanghai Academy of Spacecraft Technology of China*. Hundreds of raw experimental data for each measured parameter were acquired during a test, and the average values of all the parameters were obtained as the experimental results. The curve of the measured drawbar pull versus slip ratio is shown in Fig. 3.

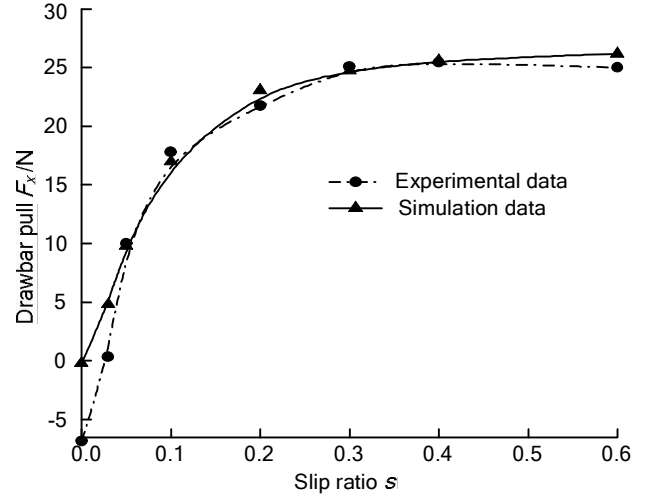


Fig. 3. Comparison of experimental and simulation results of drawbar pull versus slip ratio

### 3.3 Parameter selection and experimental verification of wheel-soil interaction model

It is important to set PAC2002 wheel-soil interaction model parameters reasonably in order to obtain a high-fidelity simulation for the rover according to the experimental data. There are many parameters in Eq. (1) that must be adjusted step by step in order to calculate the wheel-soil interaction force/moment with a high degree of precision. Detailed forms of the magic equation for calculating drawbar pull  $F_x$ , lateral force  $F_y$ , and aligning torque  $M_z$ , are as follows:

$$F_x = (B_1 F_z^2 + B_2 F_z) \cos(B_0 \arctan\{B_x X_x - (B_6 F_z^2 + B_7 F_z + B_8)[B_x X_x - \arctan(B_x X_x)]\}), \quad (2)$$

$$B_x X_x = \frac{(B_3 F_z^2 + B_4 F_z) e^{-B_5 F_z} (s + B_9 F_z + B_{10})}{B_0 (B_1 F_z^2 + B_2 F_z)}, \quad (3)$$

$$F_y = (A_1 F_z^2 + A_2 F_z) \cos(A_0 \arctan\{B_y X_y - (A_6 F_z^2 + A_7) \times [B_y X_y - \arctan(B_y X_y)]\}) + A_{11} F_z \gamma + A_{12} F_z^2 + A_{13}, \quad (4)$$

$$B_y X_y = \{A_3 (1 - A_5 |\gamma|) \sin[2 \arctan(F_z / A_4)] (\beta + A_9 F_z + A_{10} + A_8 \gamma)\} / [A_0 (A_1 F_z^2 + A_2 F_z)], \quad (5)$$

$$M_z = (C_1 F_z^2 + C_2 F_z) \cos(C_0 \arctan\{B_z X_z - (1 - C_{10} |\gamma|) (C_7 F_z^2 + C_8 F_z + C_9)[B_z X_z - \arctan(B_z X_z)]\}) + \gamma (C_{14} F_z^2 + C_{15} F_z) + C_{16} F_z + C_{17}, \quad (6)$$

$$B_z X_z = [(C_3 F_z^2 + C_4 F_z) (1 - C_6 |\gamma|) e^{-C_5 F_z} \cdot (\beta + C_{11} \gamma + C_{12} F_z + C_{13})] / [C_0 (C_1 F_z^2 + C_2 F_z)], \quad (7)$$

where  $A_0$  to  $A_{13}$ ,  $B_0$  to  $B_{10}$ , and  $C_0$  to  $C_{17}$  are adjustable parameters to ensure the fidelity of predicting the forces and moment,  $s$  is the slip ratio,  $\beta$  is the slip angle,  $\gamma$  is the camber angle, and  $F_z$  is the normal force.

The resulting parameters  $A$ ,  $B$ , and  $C$  that are adjusted according to the experimental results are shown in Tables 1 to 3. A number of other parameters were also set, including the dynamics parameters (friction, damping, rigidity, etc.) and dimension parameters.

**Table 1 Lateral force parameters**

$A_0$	2.650	$A_5$	0.005	$A_{10}$	0.371
$A_1$	12.100	$A_6$	-0.021	$A_{11}$	9.166
$A_2$	850.000	$A_7$	0.774	$A_{12}$	1.214
$A_3$	1236.000	$A_8$	0.002	$A_{13}$	-6.262
$A_4$	12.800	$A_9$	0.013		

**Table 2 Longitudinal force parameters**

$B_0$	2.373	$B_4$	76.000	$B_8$	1.200
$B_1$	9.460	$B_5$	0.089	$B_9$	0.030
$B_2$	-1490.000	$B_6$	0.004	$B_{10}$	-0.176
$B_3$	30.000	$B_7$	-0.062		

**Table 3 Aligning torque parameters**

$C_0$	-2.340	$C_6$	0.028	$C_{12}$	0.030
$C_1$	1.495	$C_7$	-0.001	$C_{13}$	-0.065
$C_2$	0.417	$C_8$	0.100	$C_{14}$	0.211
$C_3$	3.574	$C_9$	1.333	$C_{15}$	0.895
$C_4$	-0.088	$C_{10}$	2.255	$C_{16}$	-1.994
$C_5$	0.098	$C_{11}$	-0.024	$C_{17}$	-3.337

In order to verify the PAC2000 model and the parameters for predicting wheel-soil interaction, the virtual ADAMS lunar rover was controlled to move under different slip ratios by activating various resistance forces behind it. The vertical load of each wheel was set to 80N, the same as in the experimental condition.

Fig. 3 compares both the testing results and simulation results of drawbar pull for a wheel under different slip ratios. The data for drawbar pull are close to one another, except that the slip ratio is smaller than 0.05; fortunately, there is only a small difference between the slip ratios when the drawbar pull is positive with a small value. In conclusion, the PAC2000 model can predict wheel-soil interaction terramechanics with high fidelity through adjustment of the related parameters according to the experimental data.

## 4 Construction of Virtual Rough Lunar Terrain

### 4.1 Environment of lunar terrain

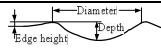


Ninety nine percent of the moon's surface terrain was formed 3 billion years ago<sup>[13]</sup>. Over such a long period, the unique environment that has no wind and strong radiation created a distinct lunar terrain.

The surface of the moon is mainly composed of lunar mare, lunar land, lunar craters, and rocks. The lunar mare is relatively flat, with a maximum gradient of 17°. The

gradient of the lunar land is larger than that of the lunar mare, with a maximum gradient of about 34°. The gradient of the inner side of a typical crater is steep, with an average gradient of 35°, though the outer side has a smaller average value of about 5°.

The craters that are widely distributed over the lunar surface can be divided into 4 types: fresh craters, young craters, mature craters, and senile craters. Table 4 shows the parameters of typical craters. It can be seen that their height is usually no more than 25% of their diameter, and that the margin height is no more than 6% of their diameter.

**Table 4 Shape of typical lunar craters**

Type of crater	Typical outline	Ratio of depth to diameter	Ratio of edge height to diameter
Fresh crater		0.23~0.25	0.022~0.06
Young crater		0.17~0.19	0.016~0.045
Mature crater		0.11~0.13	0.008~0.03

Lunar rocks are covered with soft lunar soil, which makes them be different from hard rocks due to their weathering over a long period, so that they can actually be well characterized as a soft and bumpy terrain. Table 5 shows the number of blocks in 100 m<sup>2</sup> of the landing area of surveyor 3 spacecraft.

**Table 5 Block distribution in 100 m<sup>2</sup> of lunar surface**

Height of blocks	Number of blocks
60 mm < $h$ ≤ 250 mm	100
250 mm < $h$ ≤ 500 mm	3~4
$h$ ≥ 500 mm	0.6

### 4.2 Constructing rough lunar terrain with 3DS MAX software

3DS Max software was adopted to model the rough lunar surface based on a mesh grid, as it is powerful and convenient to use. The basic terrains such as the lunar mare, land, craters, and rock, can be created according to their parameters, which can also be combined to construct a complex surface. Fig. 4 shows the lunar mare and a complex combined terrain constructed by 3DS Max.

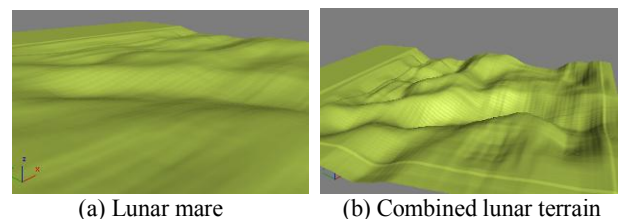


Fig. 4. 3D model of lunar terrain in 3DS Max

### 4.3 Reappearance of lunar terrain in ADAMS

The transformation of the terrain data that are used for modeling and simulation of the lunar terrain from the format of 3DS Max to that of ADAMS is a key challenge. To address this, two problems must be resolved: (1) extraction of the digital evaluation data from the lunar surface model in 3DS Max, and (2) transference of the data to a roadmap file and reproduction of the data in ADAMS without distortion.

The first problem can be solved by transferring the file formats of 3DS Max. By saving the \*.max terrain model file as an \*.ASE file, one can obtain the digital evaluation data and the relationships of their connection. The second problem is actually the interface between the 3DS Max data file and the ADAMS roadmap file that is composed of nodes data and triangular-grid units.

The so-called nodes are points whose position determines the lunar terrain, the parametric format of which is shown in Eq. (8). The first column shows the serial number of the nodes; the rest of the columns show the coordinate values in the  $x$ ,  $y$ , and  $z$  axes, respectively, with  $n$  being the number of nodes.

number_of_nodes	= $n$			
{node	$x\_value$	$y\_value$	$z\_value$	
1	$x_1$	$y_1$	$z_1$	(8)
2	$x_2$	$y_2$	$z_2$	
⋮	⋮	⋮	⋮	
$n$	$x_n$	$y_n$	$z_n$	

Adjacent nodes are connected to one another, forming triangular-grid units, as shown in Fig. 5. For example, Nodes 1, 2, and 3 compose unit A; Nodes 2, 3, and 4 compose unit B, etc. The triangular grids of the terrain are composed using this method.

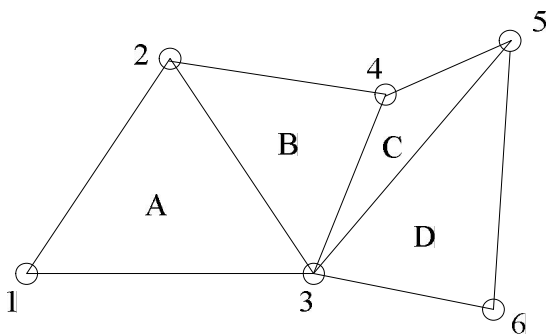


Fig. 5. Triangular-grid units of roadmap

The terrain model in 3DS Max is formed by the rectangular grids of the nodes. The \*.ASE file includes only the coordinates of points, and the lines between the coordinates of the  $x$  axis and  $y$  axis are random and iterative, which makes it much different from the triangular-grid format ADAMS roadmap file. For this reason, the data

must be transformed from a \*.ASE file to a \*.rdf file, including the triangular grid information that can be recognized by the ADAMS/Tire module. A transformation program was made with Matlab for such transformation from a \*.ASE file to a \*.rdf file. Fig. 6 shows the reappearance result of a lunar terrain in ADAMS.

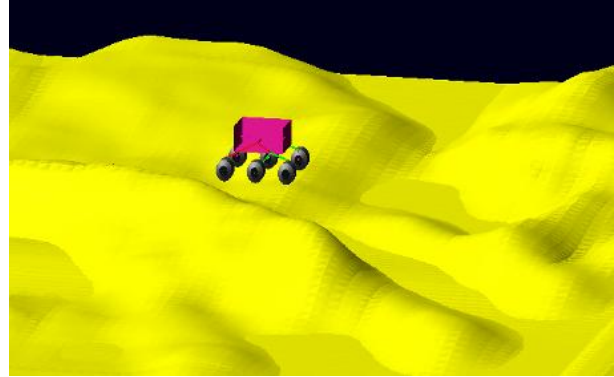


Fig. 6. Reappearance of a lunar terrain in ADAMS

## 5 Path-Following Control Strategy for Lunar Rovers on Rough Terrain

Because the lunar soil is deformable, the rover's wheels may experience longitudinal slips and side slips as the rover moves on rough terrain, causing it to lose velocity and energy and to deviate from its planned path. Such slips are usually neglected for a conventional wheeled mobile robot due to the assumption that the terrain is rigid, which is, as mentioned above, an unrealistic assumption for a lunar rover on deformable rough terrain. In order to direct a rover to move forward along a desired path, slips must be compensated for by means of control algorithms.

### 5.1 Nonholonomic kinematics model for lunar rovers

Fig. 7 shows a kinematics model of a lunar rover with side slips of both the vehicle body and the wheels. Subscript  $i$  is the number of the wheel;  $v_0$  is the linear velocity of the vehicle body;  $v_i$  is the linear velocity of the  $i$ th wheel;  $\theta_0$  is the azimuth angle of the vehicle body;  $\beta_0$  is the side slip angle of the vehicle body;  $\delta_i$  is the steering angle of the  $i$ th wheel;  $\beta_i$  is the side slip angle of the  $i$ th wheel;  $l$  is the longitudinal distance between the body center and the front or rear wheel; and  $d$  is the lateral distance between the body center and the left or right wheel. The center of the rover's body is at  $(x_0, y_0)$ , while the center of the  $i$ th wheel is at  $(x_i, y_i)$ .

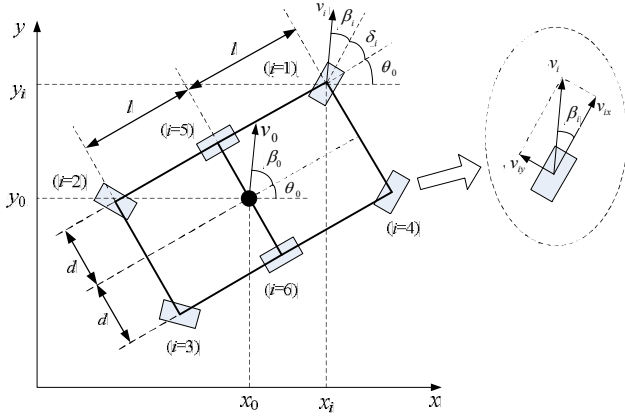


Fig. 7. Kinematics model of a lunar rover

Each steering wheel has a steering angle  $\delta_i$  and a slip angle  $\beta_i$ . The slip angle is used to measure the side slip of the wheels, and it can be calculated according to the longitudinal and side linear velocities of the  $i$ th wheel:

$$\beta_i = \arctan(v_{iy} / v_{ix}). \quad (9)$$

The kinematics model of the wheels and the rover's body can be obtained by considering the nonholonomic constraints:

$$\dot{x}_0 \sin \phi_0 - \dot{y}_0 \cos \phi_0 = 0, \quad (10)$$

$$\dot{x}_i \sin \phi_i - \dot{y}_i \cos \phi_i = 0, \quad (11)$$

where  $\phi_0 = \theta_0 + \beta_0$ ,  $\phi_i = \theta_0 + \delta_i + \beta_i$ ,  $x_i$  and  $y_i$  can be calculated by using Eqs. (12) and (13) as follows:

$$\left. \begin{aligned} x_1 &= x_0 + l \cos \theta_0 - d \sin \theta_0 \\ x_2 &= x_0 - l \cos \theta_0 - d \sin \theta_0 \\ x_3 &= x_0 - l \cos \theta_0 + d \sin \theta_0 \\ x_4 &= x_0 + l \cos \theta_0 + d \sin \theta_0 \\ x_5 &= x_0 - d \sin \theta_0 \\ x_6 &= x_0 + d \sin \theta_0 \end{aligned} \right\} \rightarrow x_i = x_0 + X_i, \quad (12)$$

$$\left. \begin{aligned} y_1 &= y_0 + l \sin \theta_0 + d \cos \theta_0 \\ y_2 &= y_0 - l \sin \theta_0 + d \cos \theta_0 \\ y_3 &= y_0 - l \sin \theta_0 - d \cos \theta_0 \\ y_4 &= y_0 + l \sin \theta_0 - d \cos \theta_0 \\ y_5 &= y_0 + d \cos \theta_0 \\ y_6 &= y_0 - d \cos \theta_0 \end{aligned} \right\} \rightarrow y_i = y_0 + Y_i. \quad (13)$$

Substituting Eqs. (12) and (13) into Eq. (11), a nonholonomic kinematics model is obtained as follows:

$$A_0 \dot{q}_0 = 0, \quad (14)$$

where

$$A_0 = \begin{bmatrix} \sin \phi_1 & -\cos \phi_1 & -l \cos(\phi_1 - \theta_0) - d \sin(\phi_1 - \theta_0) \\ \sin \phi_2 & -\cos \phi_2 & l \cos(\phi_2 - \theta_0) + d \sin(\phi_2 - \theta_0) \\ \sin \phi_3 & -\cos \phi_3 & l \cos(\phi_3 - \theta_0) - d \sin(\phi_3 - \theta_0) \\ \sin \phi_4 & -\cos \phi_4 & -l \cos(\phi_4 - \theta_0) + d \sin(\phi_4 - \theta_0) \\ \sin \theta_5 & -\cos \theta_5 & -d \sin(\theta_5 - \theta_0) \\ \sin \theta_6 & -\cos \theta_6 & -d \sin(\theta_6 + \theta_0) \end{bmatrix},$$

$$\dot{q}_0 = [\dot{x}_0 \quad \dot{y}_0 \quad \dot{\theta}_0]^T.$$

## 5.2 Path-following algorithm based on slip compensation

### 5.2.1 Path-following strategy

Fig. 8 shows a diagram of the path-following control. The present location of the rover's center is at  $P$ ;  $P_d$  is the point on the path with the shortest distance to point  $P$ ;  $\omega_0$  is the angular velocity of the rover;  $s$  is the curved distance from the starting point of the path to  $P_d$ ;  $l_e$  is the straight-line distance between  $P$  and  $P_d$ ;  $\theta_d$  is the angle from the  $x$  axis to the tangential direction of the path at point  $P_d$ , which is the desired direction of the rover;  $c$  is the curvature at point  $P_d$ ;  $\theta_e$  is the direction error calculated by  $\theta_e = \theta_0 - \theta_d$ .

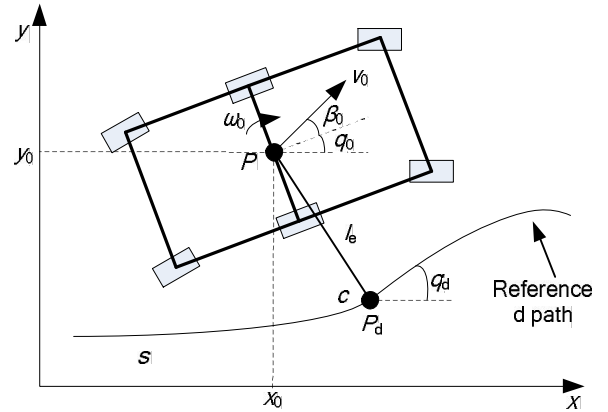


Fig. 8. Diagram of path-following control

The kinematics state equation is expressed by state variables  $s$ ,  $l_e$ , and  $\theta_e$ :

$$\begin{cases} \dot{s} = v_0 \cos(\theta_e + \beta_0) / (1 - c \cdot l_e) \\ \dot{l}_e = v_0 \sin(\theta_e + \beta_0) \\ \dot{\theta}_e = \omega_0 - c \cdot v_0 \cos(\theta_e + \beta_0) / (1 - c \cdot l_e) \end{cases} \quad (15)$$

When trying to control a rover's movement along a planned path, the errors of  $l_e$  and  $\theta_e$  should be 0. The angular velocity of the rover's body  $\omega_0$  can be controlled

in order to deduce the path-following errors. The desired angular velocity for path-following is denoted by  $u_p$ , which can be calculated using Eq. (16):

$$u_p = -k_1 v l_e - k_2 |v| \theta_e - k_3 |v| \dot{\theta}_e, \quad (16)$$

where  $k_1$ ,  $k_2$ , and  $k_3$  are the controlling parameters.

### 5.2.2 Side slip compensation strategy

Control of the rover should enable the rover to steer with an angular velocity to compensate for the side slip of the rover's body at the same time, i.e.  $\beta_0 \rightarrow 0$ . Let  $u_\beta$  denote the desired controlling angular velocity with slip compensation taken into account.  $u_\beta$  can be calculated using Eq. (17):

$$u_\beta = k_4 \beta_0 + k_5 \omega_0, \quad (17)$$

where  $k_4$  and  $k_5$  are the controlling parameters.

### 5.2.3 Control of wheels for path-following based on slip compensation

The controlling variables  $u_p$  and  $u_\beta$  can be combined to control the wheels of a rover in order to realize path-following with slip compensation<sup>[14]</sup>. For example,  $u_p$  is adopted to direct the front wheels to lead the rover along a given path, while  $u_\beta$  is adopted to control the rear wheels for slip compensation. The steering angles of the wheels can be calculated according to the nonholonomic kinematics model of the rover according to  $u_p$  and  $u_\beta$ , respectively.

#### (1) Steering control of wheels

Path-following is achieved by controlling the steering angles  $\delta_i$  ( $i = 1-4$ ). The desired steering angles  $\delta_{di}$  of all the steering wheels can be obtained according to Eq. (7):

$$\delta_{di} = \arctan(\dot{y}_i / \dot{x}_i) - \theta_d - \beta_i. \quad (18)$$

By substituting (12) and (13) into (18), one obtains:

$$\delta_{di} = \arctan \left[ \frac{\dot{y}_{d0} - \dot{Y}_i(\dot{\theta}_d)}{\dot{x}_{d0} - \dot{X}_i(\dot{\theta}_d)} \right] - \theta_d - \beta_i, \quad (19)$$

where  $\dot{X}_i$  and  $\dot{Y}_i$  are the functions of  $\dot{\theta}_d$ ,  $\dot{x}_{d0}$  and  $\dot{y}_{d0}$  are the expected linear velocities along two directions of the vehicle body, and  $\dot{\theta}_d$  is the desired angular velocity:

$$\begin{bmatrix} \dot{x}_{d0} & \dot{y}_{d0} & \dot{\theta}_d \end{bmatrix}^T = \begin{bmatrix} v_{d0} \cos \theta_d & v_{d0} \sin \theta_d & u_p(u_\beta) \end{bmatrix}^T. \quad (20)$$

In Eq. (20),  $v_{d0}$  is the desired linear velocity of the rover's body. When controlling the rover, the velocity  $v_{d0}$  and controlling parameters  $k_1 \sim k_5$  should be set using reasonable values.

#### (2) Driving control of wheels

If the wheel's longitudinal slip is neglected, the relationship between the angular velocity  $\omega_i$  and the linear velocity  $v_i$  of a wheel is

$$\omega_i = (v_i \cos \beta_i) / r, \quad (21)$$

where  $r$  is the radius of the wheel and  $v_i$  can be expressed by  $\dot{x}_i$ :

$$v_i = \dot{x}_i / \cos \phi_i. \quad (22)$$

The desired angular velocity of the wheel can be expressed by Eq. (23) according to Eq. (12):

$$\omega_{di} = \frac{[\dot{x}_{d0} + \dot{X}_i(\dot{\theta}_d)] \cos \beta_i}{r \cos \phi_i}. \quad (23)$$

The longitudinal slip ratio  $s_i$  must be considered in order to compensate for the wheel slip:

$$s_i = (r\omega_i - v_{ix}) / r\omega_i \quad (r\omega_i > v_{ix}), \quad (24)$$

where  $r\omega_i$  is the theoretical circumferential velocity of a wheel;  $v_{ix} = v_i \cos \beta_i$ , is the component of the actual velocity along the direction of a wheel. While  $s_i = 0$ , the wheel moves forward without any slip, and  $v_{ix} = r\omega_i$ ; while  $s_i = 1$ , the wheel is in a condition of constant slip with no forward movement, and at the same time,  $v_{ix} = 0$ ; while  $0 < s_i < 1$ , the wheel moves forward with longitudinal slip, and  $v_{ix} < r\omega_i$ .

The desired angular velocity of a wheel, including compensation for longitudinal slip, is

$$\hat{\omega}_{di} = \omega_{di} / [1 - (s_{ref} - s_i)], \quad (25)$$

where  $s_{ref}$  is the referenced longitudinal slip ratio while controlling a wheel, which has a value ranging from 0.1 to 0.4.

## 6 Path-Following Control Strategy for Lunar Rovers on Rough Terrain

### 6.1 Realization of joint simulation

After the following steps, the simulation model of the

lunar rover's locomotion system was finally constructed: importing of the 3D model of the lunar rover built with PRO/E and the rough lunar terrain built with 3DS Max into ADAMS; application of wheel-soil interaction mechanics to the wheels using the PAC2000 tire model of ADAMS/Tire module; and setting of parameters (tire model parameters, lunar rover parameters, gravity acceleration, and ADAMS/Solver parameters) according to the actual situation.

The method of determining the tire model is analyzed in section 3. The lunar rover's parameters include the mass, moment of inertia, wheel parameters (radius, width, and vertical rigidity  $k$ ), longitudinal distance  $L$  between the centroid and the axles of the front wheels, lateral distance  $D$  between the centroid and side wheels, etc. The gravity acceleration is set to be 1/6 of that of the earth, in a vertical-downward direction. The parameters of the ADAMS/Solver include integrator, formulation, corrector, error, outputting step, adaptivity, order of integral polynomial (Kmax), maximum iterations (Maxit), and scale.

The ADAMS/Control module is used to establish the S-function "controlled object" for the simulation model of the lunar rover's locomotion system, which is called ADAMS\_sub as shown in Fig. 9 (a), and it can be called by Matlab/Simulink. The Simulink toolbox is used to construct the joint simulation control system, the control diagram of which is shown in Fig. 9 (b). The controlled variables are the angular velocities for the six driving motors and the steering angles for the four steering motors. The feedback variables include the position, orientation, and velocity of the vehicle body.

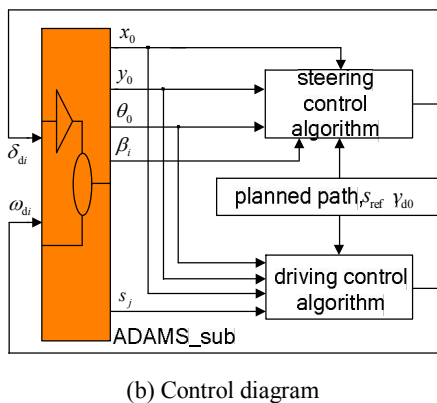
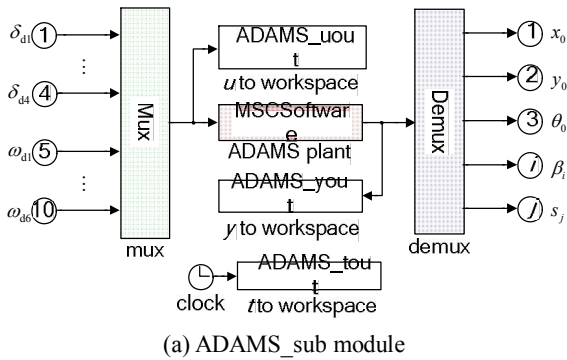


Fig. 9. Control system based on joint simulation

### 6.2 Verification of path-following algorithm

Fig. 10 shows the simulation terrain and referenced paths. The height of the barrier is 240 mm and the barrier has a gradient of 30°. Two referenced paths are planned on the terrain. Referenced path I goes from point A to point B on a line parallel to  $x$  axis. Referenced path II is composed of AC and DE, two lines parallel to  $x$  axis, and CD, a line that has a 30° included angle with  $x$  axis.

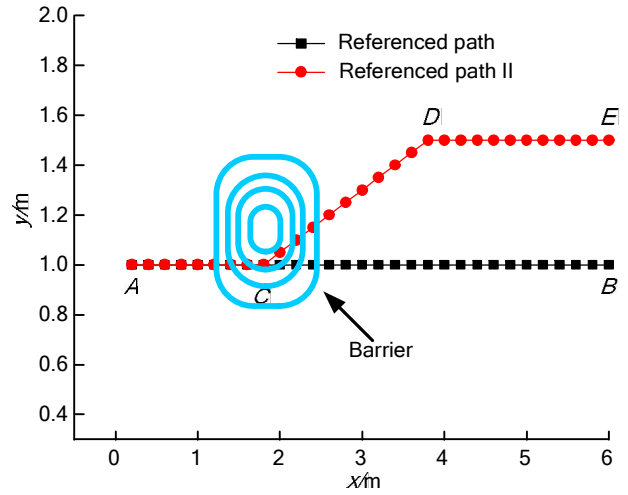


Fig. 10. Simulation terrain and referenced path

The path-following strategy uses the variable  $u_p$  to calculate the controlling parameters that enable the front wheels to follow a path, and it uses the variable  $u_\beta$  to calculate the controlling parameters for the rear wheels to compensate for side slips. If both the side and longitudinal slips are not compensated for, the side angle  $\beta_i$  and the slip ratio  $s_i$  are assumed to be zero.

After running the program to carry out a joint simulation, ADAMS/ PostProcessor can be used to play the animation and the trajectory of the centroid using the simulation results. Fig. 11 shows the simulation results for a rover that moves following referenced path II.

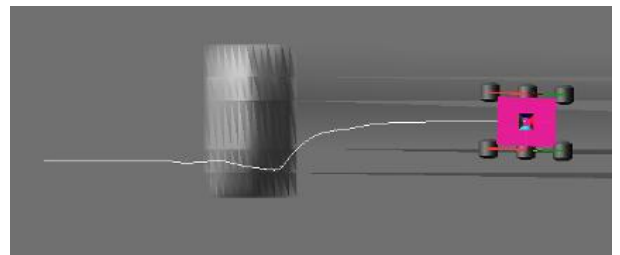
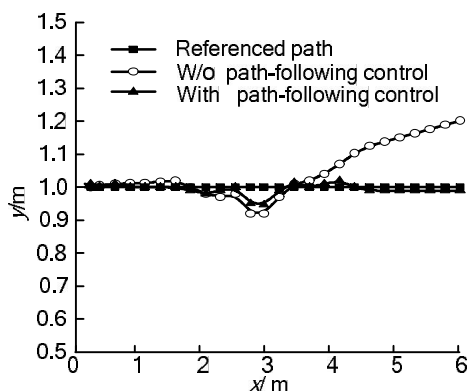


Fig. 11. Simulation results for rover following referenced path II

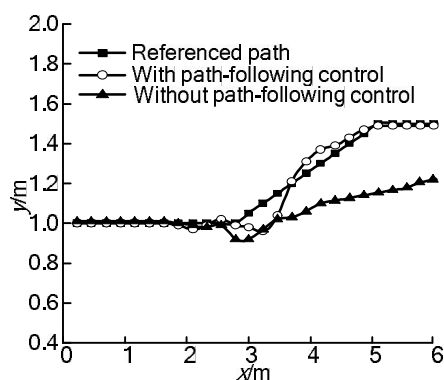
Figs. 12 (a) and (b) show a comparison of simulation results for the rover's path-following of referenced paths I and II, respectively, moving with and without a



path-following control strategy. Table 6 shows the corresponding final position and orientation errors. It can be seen from the results that the errors are large if the rover is not controlled, while the errors are small and the trajectory of the vehicle is close to the referenced path if the path-following strategy is adopted. It is thus verified that the proposed control strategy considering slip compensation is effective.



(a) Following referenced path I



(b) Following referenced path II

Fig. 12. Comparison of simulation results for path-following

**Table 6 Final position and orientation error of path-following**

Referenced path	Controlled	Position error/m	Orientation error/(°)
Referenced path I	No	0.250	3.28
	Yes	0.008	1.03
Referenced path II	No	0.250	3.28
	Yes	0.012	1.61

## 7 Conclusions

(1) The interface program developed with Matlab solves the problems of extracting data from a 3DS Max file, data transformation, and the reappearance of lunar terrain without distortion in ADAMS. Pro/E, ADAMS, and Matlab can be used to construct a virtual simulation system that integrates the features of 3D modeling,

wheel-soil interaction mechanics, dynamics analysis, mobility control, and visualization for lunar rovers.

(2) The PAC2002 tire model of the ADAMS/Tire module can be used to simulate the wheel-soil interaction mechanics. The fidelity of the model can be guaranteed by setting appropriate values for the parameters according to the experimental results. Lunar rovers experience lateral skid and longitudinal slip due to the rough lunar terrain. The proposed path-following control strategy considering slip compensation can decrease the motion deviation and enable the rover to follow the planned path. The path-following control of a lunar rover by joint simulation can provide a scheme for virtual simulation and performance analysis of rovers moving along a planned path on rough lunar terrain.

## References

- [1] DING Liang, GAO Haibo, DENG Zongquan, et al. Design of comprehensive high-fidelity/high-speed virtual simulation system for lunar rover[C]//*Proceeding of the 3rd IEEE International Conference on CIS and RAM*, Chengdu, China, Sep. 21–24, 2008: 1 118–1 123.
- [2] JAIN A, BALARAM J, CAMERON J, et al. Recent developments in the ROAMS planetary rover simulation environment[C]//*Proceedings of IEEE Aerospace Conference*, Big Sky, Montana, USA, Mar. 6–13, 2004: 861–876.
- [3] VOLPE R. Rover functional autonomy development for the mars mobile science laboratory[C]//*Proceedings of the IEEE Aerospace Conference*, Montreal, Quebec, Canada, Sep. 8–12, 2003: 643–652.
- [4] MICHAUD S, RICHTER L, PATEL N, et al. RCET: rover chassis evaluation tools[C]//*Proceedings of the 8th ESA Workshop on Advanced Space Technologies for Robotics and Automation*, ESTEC, Noordwijk, Netherlands, Nov. 2–4, 2004.
- [5] PATEL N, ELLERY A, ALLOUIS E, et al. Rover mobility performance evaluation tool (RMPET): a systematic tool for rover chassis evaluation via application of Bekker theory [C]//*Proceedings of the 8th ESA Workshop on Advanced Space Technologies for Robotics and Automation*, ESTEC, Noordwijk, Netherlands, Nov. 2–4, 2004: 251–258.
- [6] BAUER R, LEUNG W, BARFOOT T. Development of a dynamic simulation tool for the Exomars rover [C]//*Proceedings of the 8th International Symposium on iSAIRAS*, Munich, Germany, Sep. 5–8, 2005.
- [7] SOHL G, JAIN A. Wheel-terrain contact modeling in the ROAMS planetary rover simulation[C]//*Proceedings of ASME International Design Engineering Technical Conferences and Computers and Information in Engineering Conference*, Long Beach, California, USA, Sep. 24–21, 2005: 1–9.
- [8] SHANG Jianzhong, LUO Zirong, ZHANG Xinfang. Two kinds of wheeled lunar rover suspension scheme & their virtual prototype simulation[J]. *Chinese Mechanical Engineering*, 2006, 17(1): 49–51. (in Chinese).
- [9] TAO Jianguo, DENG Zongquan, HU Ming, et al. A small wheeled robotic rover for planetary exploration [C]//*Proceedings of the 1st International Symposium on Systems and Control in Aerospace and Astronautics*, Harbin, China, Jan. 19–21, 2006: 413–417.
- [10] TONG Guang. *Study on simulation platform of lunar rover based on ADAMS*[D]. Changchun: Jilin University, 2007. (in Chinese)
- [11] LIANG Bin, WANG Wei, WANG Cun'en. Initial idea on the development of China's lunar rover[J]. *Journal of International*

*Space*, 2005 (2): 22–25. (in Chinese)

- [12] WANG Wei. *Simulation study on dynamics control of a six-wheel lunar rover locomotion system*[D]. Harbin: Harbin Institute of Technology, 2002. (in Chinese)
- [13] OUYANG Ziyuan. *Introduction to lunar science*[M]. Beijing: Astronautics Press, 2005.
- [14] ISHIGAMI G, NAGATANI K, YOSHIDA K. Path following control with slip compensation on loose soil for exploration rover [C]// *IEEE/RSJ Int. Conf. on Intelligent Robots and Systems*, Beijing, China, Oct. 9–15, 2006: 5 552–5 557.

### Biographical notes

GAO Haibo, born in 1970, is currently a professor and a PhD candidate supervisor at *Harbin Institute of Technology, China*. He received his PhD degree in mechanical engineering from *Harbin Institute of Technology* in 2003. His research interests include aerospace mechanism and control.  
Email: gaohaibo@hit.edu.cn

DENG Zongquan, born in 1956, is currently a professor and a PhD candidate supervisor at *Harbin Institute of Technology, China*. His research interests include special robotics and aerospace mechanism and control.  
Email: dengzq@hit.edu.cn

DING Liang, born in 1980, is currently a lecturer at *Harbin Institute of Technology, China*. He received his PhD degree in mechanical engineering from *Harbin Institute of Technology* in 2010. His research interests include mechanics, control and simulation of mobile robots.  
Tel: +86-451-86402037-801; E-mail: liangding@hit.edu.cn

WANG Mengyu, born in 1985, received his masters degree in mechanical engineering from *Harbin Institute of Technology* in 2008.  
E-mail: wangmengyu1985@163.com